Scale Filtered Euclidean Medial Axis

Michal Postolski, Michel Couprie, Marcin Janasewski

Scale Filtered Euclidean Medial Axis *

Michał Postolski[1,2], Michel Couprie[1], and Marcin Janaszewski[2]

[1] Université Paris-Est, LIGM, Equipe A3SI, ESIEE,
Cité DESCARTES BP 99 93162 Noisy le Grand CEDEX, France
[2] Lodz University of Technology, Institute of Applied Computer Science

Abstract. We propose an Euclidean medial axis filtering method which generates subsets of Euclidean medial axis were filtering rate is controlled by one parameter. The method is inspired by Miklos', Giesen's and Pauly's scale axis method which preserves important features of an input object from shape understanding point of view even if they are at different scales. Our method overcomes the most important drawback of scale axis: scale axis is not, in general, a subset of Euclidean medial axis. It is even not necessarily a subset of the original shape. The method and its properties are presented in 2D space but it can be easily extended to any dimension. Experimental verification and comparison with a few previously introduced methods are also included.

Keywords: Filtered medial axis, discrete scale axis, shape representation, image analysis, stability

1 Introduction

The notion of medial axis has been introduced by Blum in the 60s [4]. The medial axis of an object X is composed by the centers of the balls which are included in X but which are not fully included in any other ball included in X. This set of points is, by nature, centered in the object with respect to the distance which is used to define the notion of ball.

In the literature, different methods have been proposed to compute the medial axis approximately or exactly, for instance methods relying on discrete geometry [5, 15, 16, 7], digital topology [13, 25], mathematical morphology [22], computational geometry [3, 20], partial differential equations [24], or level-sets [17]. In this work we focus on the discrete medial axis based on the Euclidean metric.

The medial axis is a very useful representation of the object and plays a major role in shape analysis in numerous applications, for example object recognition, registration or compression. From the medial axis points and associated ball radii, one can exactly reconstruct the original shape. However it can be hard or even impossible to use this tool effectively without first dealing with some problems, especially in discrete spaces and with noisy objects.

* This work has been partially supported by the "ANR-2010-BLAN-0205 KIDICO" project and Polish National Science Centre grant No. N516 480640

Firstly, the medial axis in discrete spaces has not, in general, the same topology as the original object. Solutions to this problem have been proposed by several authors, for instance [13, 25, 11]. They use discrete homotopic transformations guided and constrained by the medial axis, to obtain homotopic skeleton which contains the medial axis (see, Fig. 1). We do not consider these topological problems in the rest of the paper, and rely on this solution.

The second problem is sensitivity of the Euclidean medial axis to small contour perturbations (see, for example, Fig. 1). In other words, the medial axis is not stable under small perturbations of a shape: modifying a shape slightly (for example in terms of Hausdorff distance) can result in substantially different medial axes. This is a major difficulty when the medial axis is used in practical applications (e.g. shape recognition). A recent survey which summarises selected relevant studies dealing with this topic is presented in [2]. This fact, among others, explains why it is usually necessary to add a filtering step (or pruning step) to any method that aims at computing the medial axis and when a nonreversible but simplified description of binary objects is of interest.

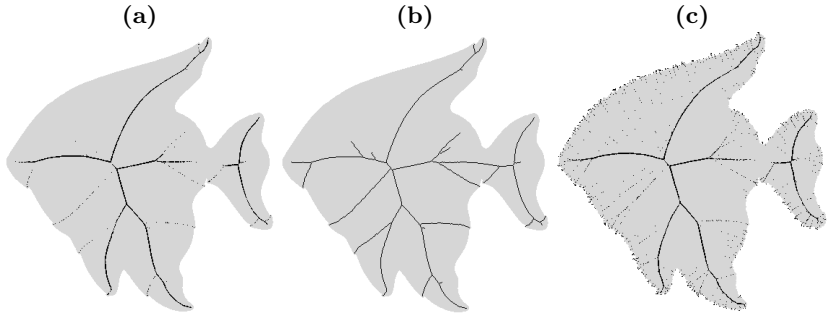

Fig. 1. (a): a shape (in gray) and its Euclidean medial axis (in black); (b) the homotopic skeleton of the shape constrained by its Euclidean medial axis; (c) the same shape, but with small amount of noise added on the contour. The medial axis of the shape (c) is much more complicated than the medial axis of the shape (a).

The simplest strategy to filter the medial axis is to keep only points which are centers of maximal balls of at least a given diameter. Different criteria can be used to locally threshold and discard spurious medial axis points or branches: see [1, 12], for methods based on the angle formed by the vectors to the closest points on the shape boundary, or the circumradius of these closest points [8, 15].

In these methods, a local information (that is, geometric information extracted from a single medial ball) is compared to a global parameter value to determine the importance of the corresponding medial axis point. However, it is well known that this local filtering can lead to remove small branches which might be important for the shape understanding (see Fig. 2) especially for shapes with features at different scales [2].

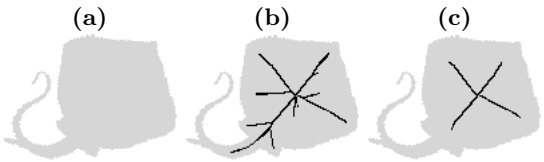

Fig. 2. (a): a shape X (in gray); (b): The filtered medial axis of X (in black) calculated by using algorithm [7]. The medial axis is not sufficiently filtered in the middle of the shape. However, we already start to loose the tail; (c) A more filtered medial axis of X. Now, the middle of the shape is well filtered. However, we lost all information about the tail.

A more complex criterion was proposed by [9]: they utilize information about ball importance in the shape with respect to all other balls by counting the number of object points inside a ball which are not covered by other balls. The medial axis point will be removed if the uncovered area of corresponding ball is too small.

In [19], the authors address this issue and propose an approach that put in relation local information and regional information, that is, the status of a ball is only influenced by the one of neighboring balls. Their method is based on the theory of the scale axis transform [14], and defines a whole family of medial representations at different levels of abstraction, called *scale axis representations* (see Fig. 3). For objects or scenes that include parts showing different scales, this method gives good results in many cases.

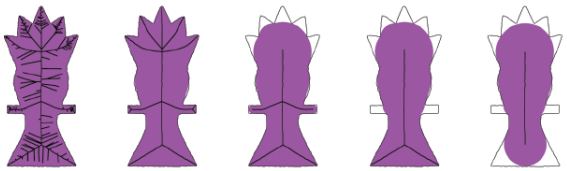

Fig. 3. Different scale axes of the same object (contoured), using different values of the scale parameter. In pink, the part of the object reconstructed from the filtered axis.

However, the scale axis representation is not free of drawbacks. The most important one is that the scale axis is not necessarily a subset of the Euclidean medial axis (see Fig. 4), it is even not necessarily a subset of the original shape.

In this paper we propose a new method for the Euclidean medial axis filtering (see section 4). Our proposition is inspired by the scale axis method (see section 3). However, as result we obtain a filtered Euclidean medial axis instead of a set of points that is not necessarily a subset of the latter. Furthermore, our method produces axes that preserve important features for shape understanding,

even if they are at different scales. Therefore, our algorithm overcomes the most important drawbacks noticed in previously presented methods following a similar approach. Moreover, the new method works in arbitrary dimensions. We evaluate experimentally its properties, and compare it with the previously introduced methods [9, 12] (see section 5).

2 Basic notions

In this section, we recall some basic geometrical and topological notions for binary images [6, 18].

We denote by $\mathbb{Z}$ the set of integers, by $\mathbb{N}$ the set of nonnegative integers, and by $\mathbb{N}_+$ the set of strictly positive integers. We denote by E the discrete space $\mathbb{Z}^d$. A point x in E is defined by $(x_1, \ldots, x_d)$ with x_i in $\mathbb{Z}$. Let $x, y \in E$, we denote by $d(x, y)$ the Euclidean distance between x and y, that is, $d(x, y) = ((x_1 - y_1)^2 + \ldots + (x_d - y_d)^2)^{1/2}$. In practice, the squared Euclidean distance is used in order to avoid floating numbers. Let $Y \subset E$, we denote by $d(x, Y)$ the Euclidean distance between x and the set Y, that is, $d(x, Y) = \min_{y \in Y}\{d(x, y)\}$. Let $X \subset E$ (the "object"), we denote by D_X the map from E to $\mathbb{R}_+ \cup \{0\}$ which associates, to each point x of E, the value $D_X(x) = d(x, \overline{X})$, where $\overline{X}$ denotes the complementary of X (the "background"). The map D_X is called the *(Euclidean) distance map of* X. Let $x \in E, r \in \mathbb{R}_+$, we denote by $B_r(x)$ the *ball of radius* r *centered on* x, defined by $B_r(x) = \{y \in E, d(x, y) < r\}$. Notice that, for any point x in X, the value $D_X(x)$ is precisely the radius of a ball centered on x and included in X, which is not included in any other ball centered on x and included in X.

Now, let us recall the notion of medial axis (see also [21, 25]). Let $X \subseteq E$. A ball $B_r(x) \subseteq X$, with $x \in X$ and $r \in \mathbb{N}_+$, is *maximal for* X if it is not strictly included in any other ball included in X. The *medial axis of* X, denoted by $\mathrm{MA}(X)$, is the set of the all couples (x, r) such that $B_r(x)$ is a maximal ball for X.

Let $X \subset E, Y \subset X$, we denote by $REDT_X(Y)$ the *reverse Euclidean distance transform* [9], defined by

$$REDT_X(Y) = \bigcup_{y \in Y} B_{D_X(y)}(y).$$

For exact and unfiltered $\mathrm{MA}(X)$ we have $X = REDT_X(MA(X))$.

3 Discrete scale axis

In this section, we adapt the notion of scale axis (see [19, 14]), originally introduced in the continuous space and implemented in a framework of unions of balls, to the case of discrete grids. We denote by $\mathbb{R}_+$ the set of strictly positive reals. Let $X \subseteq E$, $x \in X$, $r \in \mathbb{N}_+$ and $s \in \mathbb{R}_+$. The parameter s is called the *scale factor*. We denote by X_s the *multiplicatively* s*-scaled shape*, defined by

$X_s = \bigcup_{(x,r)\in MA(X)} B_{rs}(x)$. For $s \geqslant 1$, we denote by $\mathrm{SAT}_s(X)$ the *s-scale axis transform* of X, defined by

$$\mathrm{SAT}_s(X) = \{(x, r/s) \mid (x, r) \in MA(X_s)\}.$$

The original algorithm to compute discrete scale axis, given by [19] in the framework of union of balls (UoBs), can be straightforwardly adapted to the case of $\mathbb{Z}^d$ as follows. First, calculate the Euclidean medial axis of X. To do so, we use an efficient algorithm presented in [9]. Then multiply radius of each medial ball by the chosen scaling factor s.

In consequence small medial balls are covered completely by larger nearby balls since they are not important. On the other hand, small balls without larger balls in their neighborhood are not covered and will be preserved.

Next step is to reconstruct object X_s based on scaled radius values. Reconstruction can be made efficiently by reverse Euclidean distance transform (see section 2). Computing the medial axis of X_s achieves the simplification and $MA(X_s)$ will be free of all covered balls, since these do not touch the boundary anymore and are thus no longer maximal. For $s = 1$, the scale axis is identical to unfiltered Euclidean medial axis. With increasing s, the scale axis gradually ignores less important features of X leading to successive simplifications of X_s and the scale axis structure.

The final step of the algorithm consists of rescaling the medial balls of $\mathrm{MA}(X_s)$ by a factor $1/s$ to obtain the scale axis of X. Finally, discrete scale axis algorithm can be presented in the following pseudocode:

Algorithm 1 DiscreteScaleAxis(**Input** X,s **Output** $SAT_s(X)$)

01. Compute $MA(X)$
02. Reconstruct X_s
03. Compute $MA(X_s)$
04. Compute $SAT_s(X)$

All four steps of DiscreteScaleAxis algorithm can be calculated in linear time in relation to $\#X$, $\#X_s$, $\#X_s$ and $\#MA(X_s)$ respectively, where $\#X$ stands for cardinality of X. Therefore, computational complexity of the algorithm is $O(\#X_s)$.

4 The scale filtered medial axis

The crucial part of the method presented in the previous section, which is a source of problems ($\mathrm{MA}(X_s) \nsubseteq \mathrm{MA}(X)$), is the reconstruction part after medial balls scaling and the need for generating a new medial axis from the scaled object (see Fig. 4). On the other hand, at first sight, this is the most important part of the algorithm since the medial axis simplification occurs in this part.

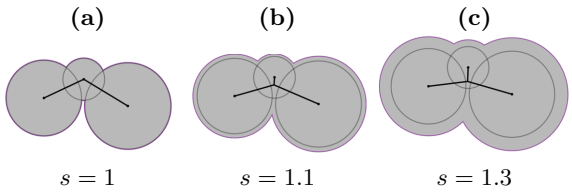

Fig. 4. (a): a shape X (in gray) and its Euclidean medial axis $MA(X)$ (in black); (b): the multiplicatively 1.1-scaled shape of X and its 1.1-scaled axis; (c): the multiplicatively 1.3-scaled shape of X and its 1.3-scaled axis. In (b, c) we can see that scale axes are not subsets of $MA(X)$. In both cases, an additional branch even appears.

To filter MA(X) by removing centers of unimportant medial balls one must avoid reconstruction part and hold simplification property at the same time. Therefore, to solve this problem we assume that to make efficient filtration we just need to decide which MA(X) points are not important and should be removed. Therefore, we do not generate a new object X_s and its MA(X_s). In this way we obtain filtered Euclidean medial axis of X which is a subset of MA(X).

This informal discussion motivates the following definition of the Scale Filtered Euclidean Medial Axis (SFEMA).

Let $x \in X, r \in \mathbb{N}_+$. We denote by $B_r^X(x)$ the intersection of $B_r(x)$ with X, that is, $B_r^X(x) = \{y \in X \mid d(x,y) < r\}$.

Definition 1. *Let $X \subseteq E$, and $s \in \mathbb{R}, s \geqslant 1$. We denote by $SFEMA_s(X)$ the Scale Filtered Euclidean Medial Axis of X defined by*

$$SFEMA_s(X) = \{(x,r) \in MA(X) \mid B_{rs}^X(x) \nsubseteq \bigcup_{(y,t)\in MA(X), t>r} B_{ts}^X(y)\}.$$

Below, we give an algorithm to compute $SFEMA_s(X)$ of a given object $X \subseteq E$.

The algorithm in line 02 performs sorting of medial axis elements, linearly in time using a counting sort [10]. In the following lines the algorithm performs two loops. The first one starts in line 04 and does $\#X$ iterations. The next, nested loop, starts in line 06 and in worst case performs $\#MA(X)$ iterations. Summarizing, computational complexity of SFEMA is $O(\#X\#MA(X))$.

Examples of $SFEMA_s(X)$ for different scale factors s_i, are shown in Fig. 5.

Let us analyze properties and the major differences between the Miklos's [19] s-scale axis and our s-scale filtered Euclidean medial axis. The most important property is that $SFEMA_s(X)$ consists of $MA(X)$ points only, that is, for all $s \geqslant 1$: $SFEMA_s(X) \subseteq MA(X)$. This property (inclusion property, for short) is essential in many applications of the medial axis. In Fig.4 we have shown an example of the Miklos's scale axis where an additional branch even appears after filtering. Fig.6 shows another problem. The scale axis is too much simplified, looses important features of the object and is not included in the object. However,

Algorithm 2 SFEMA(**Input** X,s **Output** H)

```
01.  H ← ∅
02.  MA(X) ← EuclideanMedialAxis(X)
03.  Let (x_1, r_1), ..., (x_n, r_n) denote the elements of MA(X)
     sorted in decreasing order of radii, that is, r_1 ⩾ ... ⩾ r_n
04.  foreach p ∈ X do
05.      i ← 1
06.      while i ⩽ n and d(x_i, p) > sr_i do i ← i + 1 end
07.      If i ⩽ n then
08.          H ← H ∪ {(x_i, r_i)}
09.      end
10.  end
11.  return H
```

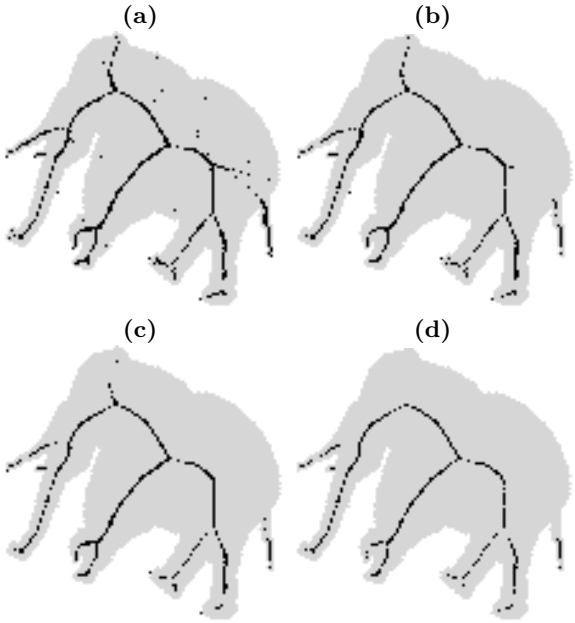

Fig. 5. (a): a shape X (in gray) and its Euclidean medial axis (in black); (b, c, d): the same shape and its $SFEMA_{1.1}(X)$, $SFEMA_{1.4}(X)$, $SFEMA_{1.6}(X)$, respectively. In all cases the elephant's tail, trunk, tusks and legs were considered as important and were not removed.

s-scale filtered medial axis holds inclusion property and permits to reconstruct the most of the original object.

The second interesting property relies on the notion of s-scale ball. If we want to simplify the object, using Miklos's scale axis, for example, by removing

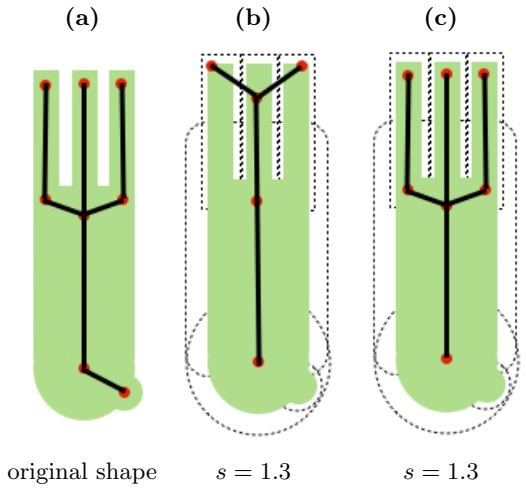

Fig. 6. (a): a set X (in green) and its $MA(X)$ (in black); (b): the 1.3-scale axis of X; (c): the 1.3-scale filtered medial axis of X.

a medial ball $B_r(x), x \in X$, the scale factor should be big enough that ball $B_{rs}(x)$ is included in one of other medial balls, that is, $B_{rs}(x) \subset B_{rs}(y), y \in X$ (see Fig.7c), or in a union of such balls. In our algorithm, since we use notion of s-scaled ball, we only test inclusion inside X (see Fig.7b). This allows us to use smaller scale factor. Therefore, we have better ability to control resulting s-scale filtered Euclidean medial axis.

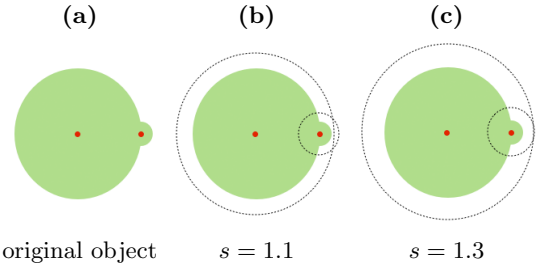

Fig. 7. (a): a set X (in green) and its $MA(X)$ (red dots); (b): multiplicatively scaled medial balls. The smaller ball is not fully covered by the bigger one after scaling. In scale axis representation both balls will be preserved. However, the bigger ball includes the smaller one inside set X. Therefore, the smaller ball will not exist in $SFEMA_s(X)$; (c): multiplicatively scaled medial balls. The smaller ball is included in the bigger one. Therefore, it is neither in the scale axis nor in $SFEMA_s(X)$

.

5 Experiment methodology and results

In this section, we compare qualitatively and quantitatively properties of three medial axis filtering algorithms: discrete λ-medial axis (DLMA) [7], Euclidean medial axis filtered with the use of bisector function (BisEMA) [12] and SFEMA. In our experiments we use shapes from Kimia's database [23].

We first introduce some notions which help us to compare the algorithms. As it was stated in sec. 2, considering the exact and unfiltered MA(X), the reverse Euclidean distance transform of $MA(X)$ is equal to X. However, this property is no longer true if we consider filtered medial axes e.g. DLMA, BisEMA, SFEMA. Therefore, it is interesting to measure how much information about the original object is lost when we perform filtering. Considering a subset Y of $MA(X)$, we define:

$$R_X(Y) = \frac{|X \setminus REDT_X(Y)|}{|X|}.$$

We call $R_X(Y)$ the *(normalised) residuals of* Y. Residuals give us a numerical evaluation of *reconstruction error*. Now we can set Y to different filtered medial axes, e.g. by using different methods or filtering parameters, and then evaluate which filtration is better in respect of ability to reconstruct the original object. The result $R_X(Y)$ is a real value between 0 (perfect reconstruction) and 1 (bad reconstruction).

The normalised residuals factor is not enough to assess the quality of a filtered medial axis. It is difficult to compare different algorithms because filtering parameters of the algorithms have different meanings, therefore we introduce the *normalised medial axis size* NS.

Let denote by $NS_X(Y)$ *normalised medial axis size* defined as a ratio of the number of the medial axis points to the number of object points: $NS_X(Y) = \#Y/\#X$.

Now we can compare normalised residuals obtained using different methods for the same NS. In other words, we replace the parameters of the different medial axis filtering algorithms by only one parameter (NS), which ensures a fair comparison.

Figure 8 presents DLMA, BisMA and SFEMA of an exemplary shape, extracted for several values of normalised residuals. The figure shows that SFEMA of smaller size than DLMA results in the same value of R. Moreover, in contrast to DLMA, SFEMA represents the most important fragments of an input object in different scales (see the tail in the last column of Fig. 8). SFEMA algorithm filters better than BisEMA some unimportant points close to the border of the sea devil main body.

The next important property of SFEMA can be concluded from Fig. 9 which shows accuracy of the object representation by filtered medial axis for different NSs. One can see that SFEMA obtains the smallest residuals value for most NSs. In other words SFEMA results with filtered medial axes which the most accurately represent the input object in different scales. Moreover Fig. 9 shows

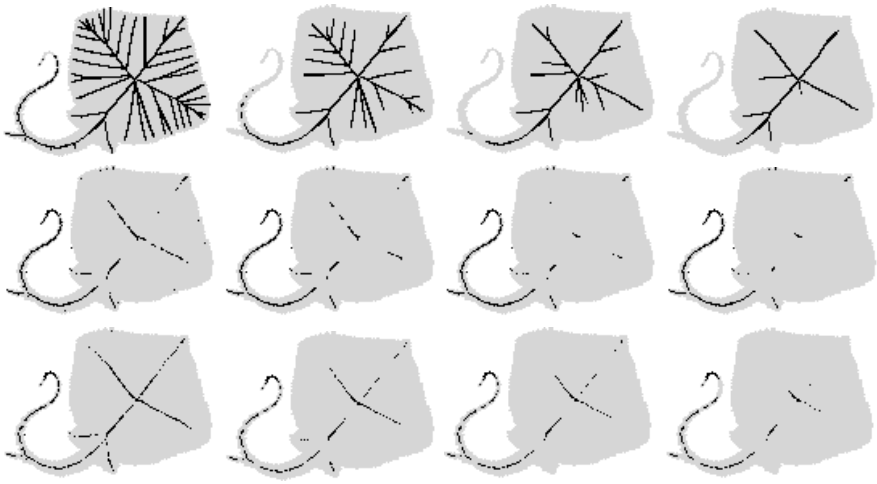

Fig. 8. Medial axes in black superimpose to input object in grey color. Consecutive rows (from left to the right) contain results for DLMA, BisEMA and SFEMA respectively. Columns contain results for different values of normalised residuals: 0.01, 0.03, 0.05, 0.1 respectively.

that SFEMA algorithm generates many more different filtered medial axes than DLMA algorithm does. This property is important when we are interested in multiscale representation of an input object. In this case, the number of different filtered medial axes generated with DLMA algorithm might be not enough. The above conclusions confirm results presented in Table 1. SFEMA has obtained the lowest mean normalised residuals for all NSs.

Table 1. Average normalised residuals calculated for 18 representative shapes from Kimia's database [23]. Lowest values are highlighted in gray

	2D		
NS	2%	3%	5%
DLMA	0.2566	0.1717	0.0996
BisEMA	0.3268	0.1183	0.0775
SFEMA	0.0991	0.0562	0.0112

6 Conclusions

The article presents a new method for Euclidean medial axis filtering which possesses the following properties:

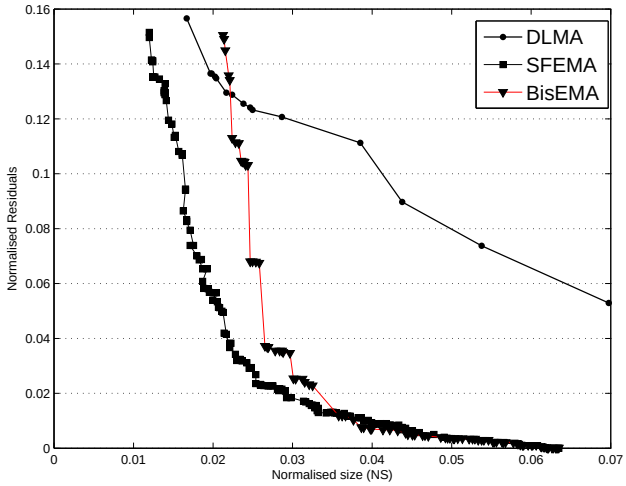

Fig. 9. Residuals as a function of normalised medial axis size for DLMA(curve with circles), BisEMA(curve with triangles) and SFEMA(curve with squares). Results generated for sea devil image (see Fig 8). Each marker (triangle, circle and square) represents parameters of one filtered medial axis. Lines has been added only to emphasise the trend of measurements

- generates subsets of Euclidean medial axis,
- filtering is based on only one parameter,
- generates filtered medial axes which preserve important parts of an input object in different scales,
- obtains smaller normalised residuals than other compared medial axis filtering algorithms,
- computation complexity of the algorithm is $O(\#X\#MA(X))$.

Future works will include the design of a more formalised framework for quantitative comparison of filtered medial axes at different scales. Using this framework the authors plan to perform more tests for 2D and 3D objects.

References

1. Attali, D., Sanniti di Baja, G., Thiel, E.: Pruning discrete and semicontinuous skeletons. In: Conference on Image Analysis and Processing. LNCS, vol. 974, pp. 488–493. Springer (1995)
2. Attali, D., Boissonnat, J.D., Edelsbrunner, H.: Stability and computation of the medial axis — a state-of-the-art report. In: Mathematical Foundations of Scientific Visualization, Computer Graphics, and Massive Data Exploration, pp. 109–125. Springer-Verlag (2009)

3. Attali, D., Lachaud, J.: Delaunay conforming iso-surface, skeleton extraction and noise removal. Computational Geometry: Theory and Applications 19, 175–189 (2001)
4. Blum, H.: A transformation for extracting new descriptors of shape. In: Models for the Perception of Speech and Visual Form, pp. 362–380. MIT Press (1967)
5. Borgefors, G., Ragnemalm, I., di Baja, S.: The euclidean distance transform: finding the local maxima and reconstructing the shape. In: Procs. of the 7th Scand. Conf. on image analysis. vol. 2, pp. 974–981 (1991)
6. Chassery, J., Montanvert, A.: Géometrie discrète. Hermès (1991)
7. Chaussard, J., Couprie, M., Talbot, H.: Robust skeletonization using the discrete lambda-medial axis. Pattern Recognition Letters 32(9), 1384–1394 (2011)
8. Chazal, F., Lieutier, A.: The λ-medial axis. Graphical Models 67(4), 304–331 (2005)
9. Coeurjolly, D., Montanvert, A.: Optimal separable algorithms to compute the reverse euclidean distance transformation and discrete medial axis in arbitrary dimension. IEEE Trans. Pattern Anal. Mach. Intell. 29(3), 437–448 (2007)
10. Cormen, T.H., Leiserson, C., Rivest, R.: Introduction to algorithms. MIT Press (1990)
11. Couprie, M., Bertrand, G.: Discrete topological transformations for image processing. In: Brimkov, V.E., Barneva, R.P. (eds.) Digital Geometry Algorithms, Lecture Notes in Computational Vision and Biomechanics, vol. 2, chap. 3, pp. 73–107. Springer (2012)
12. Couprie, M., Coeurjolly, D., Zrour, R.: Discrete bisector function and euclidean skeleton in 2d and 3d. Image Vision Comput. 25(10), 1543–1556 (2007)
13. Davies, E.R., Plummer, A.P.N.: Thinning algorithms: A critique and a new methodology. Pattern Recognition 14(1-6), 53–63 (1981)
14. Giesen, J., Miklos, B., Pauly, M., Wormser, C.: The scale axis transform. In: Proceedings of the 25th annual symposium on Computational geometry. pp. 106–115. SCG '09, ACM, New York, NY, USA (2009)
15. Hesselink, W., Roerdink, J.: Euclidean skeletons of digital image and volume data in linear time by the integer medial axis transform. IEEE Trans. on PAMI 30(12), 2204–2217 (2008)
16. Hulin, J.: Axe Médian Discret : Propriétés Arithmétiques et Algorithmes. Ph.D. thesis, Université Aix-Marseille II, Marseille (2009)
17. Kimmel, R., Shaked, D., Kiryati, N., Bruckstein, A.M.: Skeletonization via distance maps and level sets. Computer Vision and Image Understanding 62, 382–391 (1995)
18. Kong, T.Y., Rosenfeld, A.: Digital topology: Introduction and survey. Computer Vision, Graphics, and Image Processing 48(3), 357–393 (1989)
19. Miklos, B., Giesen, J., Pauly, M.: Discrete scale axis representations for 3d geometry. ACM Trans. Graph. 29, 101:1–101:10 (July 2010)
20. Ogniewicz, R., Kübler, O.: Hierarchic voronoi skeletons. Pattern Recognition 28(33), 343–359 (1995)
21. Rosenfeld, A.: Digital image processing. Academic Press (1982)
22. Serra, J.: Image analysis and mathematical morphology. Academic Press (1982)
23. Sharvit, D., Chan, J., Tek, H., Kimia, B.: Symmetry-based indexing of image databases. Journal of Visual Communication and Image Representation 9(4), 366–380 (1998)
24. Siddiqi, K., Bouix, S., Tannenbaum, A., Zucker, S.: The hamilton-jacobi skeleton. In: International Conference on Computer Vision (ICCV). pp. 828–834 (1999)
25. Talbot, H., Vincent, L.: Euclidean skeletons and conditional bisectors. In: Proceedings of VCIP'92, SPIE. vol. 1818, pp. 862–876 (1992)